

Diamond Coating in Accelerator Structure

Xintian Eddie Lin

Presented at Advanced Accelerator Concepts Workshop,
Baltimore, MD, 7/6/98—7/11/98

Stanford Linear Accelerator Center, Stanford University, Stanford, CA 94309

Work supported by Department of Energy contract DE-AC03-76SF00515.

Diamond Coating in Accelerator Structure

Xintian E. Lin¹

Abstract. The future accelerators with 1 GeV/m gradient will give rise to hundreds of degrees instantaneous temperature rise on the copper surface. Due to its extraordinary thermal and electric properties, diamond coating on the surface is suggested to remedy this problem. Multi-layer structure, with the promise of even more temperature reduction, is also discussed, and a proof of principle experiment is being carried out.

I INTRODUCTION

The quest for high accelerating gradient, on the order of 1 GeV/m, calls for the development at high frequency. While peak power requirement, breakdown voltage scaling with frequency is favorable at higher frequency, The pulsed temperature rise of a 1 GeV/m machine is still prohibitively high. Basically the heat generated by wall loss from microwave pulse diffuses slowly into the metal and local temperature increases with the one half power of the pulse duration. Diamond coating on the metal inner surface was suggested [1] to remove the heat away. The configuration is illustration in Fig. 1. Diamond being the hardest known material also has the

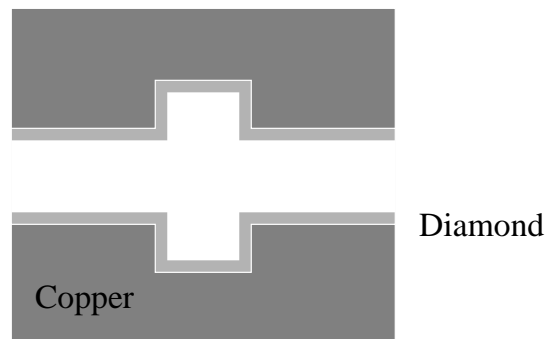


FIGURE 1. Surface coating in accelerator cavity.

highest thermal conductivity of 2000 W/m·K at room temperature, 5 times that of copper. The commercial success of Chemical Vapor Deposition (CVD) in artificial diamond synthesis makes it economically feasible to be used in many applications. One of them is heat sink in high power semiconductor device to lower its working

¹) Work supported by the Department of Energy, contract DE-AC03-76SF00515.

temperature, and thus raise the reliability. In our application, the heat generated on the metal surface diffuses away through 2 thermal paths instead of one: one into metal and one into diamond. As long as diamond coating is substantially thicker than the diffusion length $\lambda = \sqrt{KT_p/C_v\rho}$ in diamond, the heat will not be reflected from diamond-vacuum interface until after the microwave pulse is over. The quantities K , C_v and ρ are the thermal conductivity, specific heat and density of diamond respectively. The pulse length is represented by T_p . With a 16 ns pulse, $\lambda = 4 \mu m$. The coating layer essentially acts as a fast heat diffuser and heat reservoir to temporarily store the energy.

II COATINGS

The following sections present a detail analysis of the thermal property of such layered system, and electric property will be mentioned briefly.

A thermal diffusion

Thermal diffusion in multi-layer system is common in applications ranging from heat spread and heat sinks. There are many papers on this very subject. But most of them calculate the steady-state equilibrium distribution, a solution of Helmholtz equation. This section provides the solution of the time dependent thermal diffusion equation in a multi-layered system.

The governing equation for heat diffusion is

$$\rho C_v \frac{\partial T(t, \vec{x})}{\partial t} - K \nabla^2 T(t, \vec{x}) = P(t, \vec{x}), \quad (1)$$

where ρ , C_v and K are the density, specific heat and thermal conductivity of the material respectively. The power density is denoted by P .

Laplace transforming Eq. 1, we have

$$\rho C_v (p\bar{T} - T(0+, \vec{x})) - K \nabla^2 \bar{T} = \bar{P}, \quad (2)$$

where the Laplace transform is defined as

$$\bar{T} \equiv L(T) = \int_0^\infty T e^{-pt} dt, \quad (3)$$

and the result

$$L\left(\frac{\partial T}{\partial t}\right) = pL(T) - T(0+) \quad (4)$$

is used to obtain Eq. 2.

To simplify the problem, we consider only the case of one spatial dimension. The operator ∇^2 , therefore reduces to $\frac{\partial^2}{\partial x^2}$. We assume the initial condition $T(0+, x) = 0$, which leads to

$$-K \frac{\partial^2 \bar{T}}{\partial x^2} + \rho C_v p \bar{T} = \bar{P}. \quad (5)$$

The homogeneous solution of Eq. 5 is then

$$\bar{T} = ae^{-\sqrt{p/D}x} + be^{\sqrt{p/D}x}, \quad (6)$$

where diffusivity is defined as $D \equiv K/\rho C_v$ and a and b are constants.

In a two medium system, illustrated in Fig. 2, the temperature distribution T_1

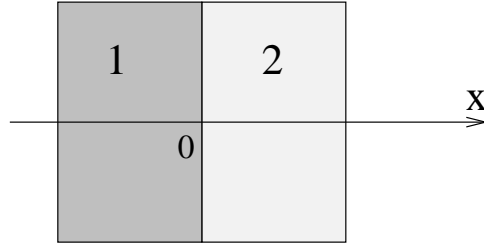


FIGURE 2. Heat diffusion in two medium with source at the interface.

and T_2 in the two regions has the form

$$\left. \begin{aligned} \bar{T}_1 &= a_1 e^{\sqrt{p/D_1}x} \\ \bar{T}_2 &= a_2 e^{-\sqrt{p/D_2}x} \end{aligned} \right\} \quad (7)$$

as a result of the boundary condition at infinity. The heat source \bar{P} is assumed to be a delta function $\delta(x)$. Continuity at $x = 0$ requires that $a_1 = a_2$. Integrating Eq. 5 from $x = 0^-$ to $x = 0^+$ yields

$$(-K_2) \frac{\partial T_2}{\partial x} \Big|_{0^+} - (-K_1) \frac{\partial T_1}{\partial x} \Big|_{0^-} = \int_{0^-}^{0^+} \bar{P} = 1. \quad (8)$$

Substituting Eq. 7 in Eq. 8, we obtain

$$a_1 = \frac{1}{1 + Z_2/Z_1} \frac{1}{Z_1 \sqrt{p}}, \quad (9)$$

where we defined the heat wave impedance $Z_i \equiv \sqrt{\rho_i C_{vi} K_i}$. Using the property

$$L^{-1} \left(\frac{1}{\sqrt{p}} e^{-a\sqrt{p}} \right) = \frac{1}{\sqrt{\pi t}} e^{-a^2/4t}, \quad (10)$$

we obtain the temperature distribution in the medium

$$T_i = \frac{1}{1 + Z_2/Z_1} \frac{1}{Z_1 \sqrt{\pi t}} e^{-x^2/4D_i t}. \quad (11)$$

The solution is the Green's function of diffusion equation with source at $x = 0$. Eq. 11 can be understood in terms of heat generated at $x = 0$ being shared in the two medium according to their respective thermal wave impedances Z_i . When the two media are the same, Eq. 11 reduces to the well known result for the Green's function in a uniform medium

$$G(x, x', t, t') = \frac{1}{\sqrt{4\pi}} \frac{1}{\sqrt{K\rho C_v(t-t')}} e^{-(x-x')^2/4D(t-t')} \quad (12)$$

Since the skin depth at 91 GHz is only 0.22 μm in copper, the diffusion length of a 16 ns pulse $\sqrt{D_1 T_p} = 1.4\mu\text{m}$ is much larger. Thus to a good approximation, we may assume all the heat is generated at the interface $x = 0$. We will deal with finite skin depth effect later. The surface temperature rise is then

$$T = \frac{1}{1 + Z_2/Z_1} \frac{2P_0 T_p}{\sqrt{\pi K_1 \rho_1 C_{v1} T_p}} \quad (13)$$

after integrating Eq. 11 over a square pulse of length T_p . The surface power flux is represented by P_0 . With diamond coating on copper, the peak temperature is $(1+Z_2/Z_1)^{-1} = 0.36$ times that of copper alone. The diamond thermal conductivity, density and specific heat are 1800 W/m·K, 3.54 kg/m³ and 674 J/kg·K respectively; and those of copper are 401 W/m·K, 8.96 kg/m³ and 385 J/kg·K.

B three-layer model

The above estimation assumes an infinite thick diamond layer. One way of modeling the finite diamond coating thickness is a three-layer configuration, illustrated in Fig. 3. Assuming the heat source is located at $x = x_1$, the temperature \bar{T}_i can

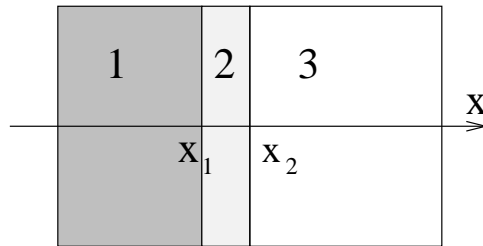


FIGURE 3. Three-layer coating model. The heat source is assumed to be located at $x = x_1$.

be expressed as

$$\left. \begin{aligned} \bar{T}_1(x, p) &= a_1 e^{\sqrt{p/D_1}(x-x_1)} \\ \bar{T}_2(x, p) &= a_2 e^{-\sqrt{p/D_2}(x-x_1)} + b_2 e^{\sqrt{p/D_2}(x-x_1)} \\ \bar{T}_3(x, p) &= a_3 e^{\sqrt{p/D_3}(x-x_2)} \end{aligned} \right\} \quad (14)$$

The continuity of temperature and heat flux at $x = x_2$ requires

$$\left. \begin{aligned} a_2 e^{-\sqrt{p/D_2}(x_2-x_1)} + b_2 e^{\sqrt{p/D_2}(x_2-x_1)} &= a_3 \\ a_2 e^{-\sqrt{p/D_2}(x_2-x_1)} - b_2 e^{\sqrt{p/D_2}(x_2-x_1)} &= \frac{Z_3}{Z_2} a_3 \end{aligned} \right\} \quad (15)$$

Solving Eq. 15, we obtain

$$S_{22} \equiv \frac{b_2}{a_2} = \frac{1 - Z_3/Z_2}{1 + Z_3/Z_2} e^{-2\sqrt{p/D_2}(x_2-x_1)}. \quad (16)$$

Similarly, at $x = x_1$ we have

$$\left. \begin{aligned} a_2 + b_2 &= a_1 \\ k_2(-a_2\sqrt{\frac{p}{D_2}} + b_2\sqrt{\frac{p}{D_2}}) - k_1 a_1 \sqrt{\frac{p}{D_1}} &= -1 \end{aligned} \right\} \quad (17)$$

Combining Eq. 16 and 17, we can solve for a_1, a_2, b_2 and a_3 :

$$\left. \begin{aligned} a_1 &= \frac{1}{\sqrt{p}Z_1(1+Z_2/Z_1)} \frac{1+S_{22}}{1+\alpha_{12}S_{22}} \\ a_2 &= \frac{1}{\sqrt{p}Z_1(1+Z_2/Z_1)} \frac{1}{1+\alpha_{12}S_{22}} \\ b_2 &= \frac{1}{\sqrt{p}Z_1(1+Z_2/Z_1)} \frac{S_{22}}{1+\alpha_{12}S_{22}} \\ a_3 &= \frac{1}{\sqrt{p}Z_1(1+Z_2/Z_1)} \frac{e^{-\sqrt{p/D_2}(x_2-x_1)}}{1+\alpha_{12}S_{22}} \frac{2}{1+Z_3/Z_2} \end{aligned} \right\} \quad (18)$$

where

$$\alpha_{12} = \frac{1 - Z_2/Z_1}{1 + Z_2/Z_1}. \quad (19)$$

The temperature at $x = x_1$ follows

$$\bar{T}_1(x_1, p) = a_1 = \frac{1}{\sqrt{p}Z_1(1+Z_2/Z_1)} (1+S_{22}) \sum_{n=0}^{\infty} (-\alpha_{12}S_{22})^n, \quad (20)$$

where we have expanded the denominator. Eq. 20 can be simplified further to read

$$\bar{T}_1(x_1, p) = \frac{1}{(1+Z_2/Z_1)} \frac{1}{Z_1\sqrt{p}} \left[1 + \sum_{n=1}^{\infty} \left(1 - \frac{1}{\alpha_{12}}\right) (-\alpha_{12})^n \alpha_{23}^n e^{-2n\sqrt{p/D_2}\Delta x} \right], \quad (21)$$

where $\alpha_{23} = (1 - Z_3/Z_2)/(1 + Z_3/Z_2)$ and $\Delta x = x_2 - x_1$. Utilizing Eq. 10, we obtain the temperature at x_1

$$T_1(x_1, t) = \frac{1}{1+Z_2/Z_1} \frac{1}{\sqrt{K_1\rho_1 C_{v1}\pi t}} \left[1 + \sum_{n=1}^{\infty} \left(1 - \frac{1}{\alpha_{12}}\right) (-\alpha_{12})^n \alpha_{23}^n e^{-4n^2\Delta x^2/4D_2t} \right]. \quad (22)$$

Compared to Eq. 11 with $x = 0$, the finite thickness of medium 2 gives a correction factor; each term under the sum represents the multiple reflection of heat wave

between 2 interfaces. Integrating Eq. 22 with a square pulse, we obtain the surface temperature

$$T = \frac{1}{1 + Z_2/Z_1} \frac{2P_0 T_p}{\sqrt{\pi K_1 \rho_1 C_{v1} T_p}} [1 + \alpha_c] \quad (23)$$

where the coating thickness correction factor

$$\alpha_c = \sum_{n=1}^{\infty} \left(1 - \frac{1}{\alpha_{12}}\right) (-\alpha_{12})^n \alpha_{23}^n (e^{-n^2 \Delta x_s^2} - n \Delta x_s \sqrt{\pi} \operatorname{erfc}(n \Delta x_s)), \quad (24)$$

and the scaled coating thickness $\Delta x_s = \Delta x / \sqrt{D_2 T_p}$.

The value of α_c , plotted in Fig. 4 for finite diamond thickness on copper, naturally

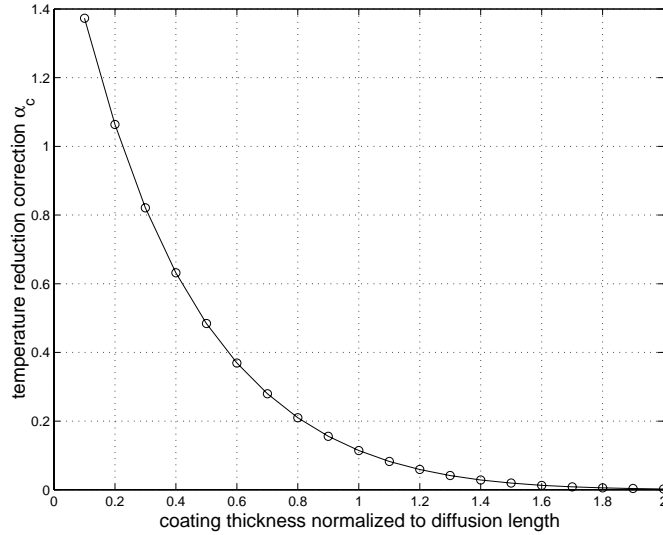


FIGURE 4. The correction factor α_c plotted as a function of coating thickness, which is normalized to diffusion length $\sqrt{D_2 T_p}$.

approaches zero as Δx becomes large. But even with a coating thickness of 1.5 and 2 diffusion lengths, the correction is only 2% and 0.2% respectively.

C RF skin depth effect

The effect of RF skin depth can also be calculated from the three-layer model if we assume medium 1 and 2 are the same metal and medium 3 is diamond. From Eq. 18, we obtain

$$\bar{T}(x_2, p) = a_3 = \frac{1}{1 + Z_2/Z_1} \frac{1}{\sqrt{p} Z_1} e^{-\sqrt{p/D_1} \Delta x}, \quad (25)$$

where the subscript is renumbered to suit Fig. 5. Taking the inverse Laplace transform, we get

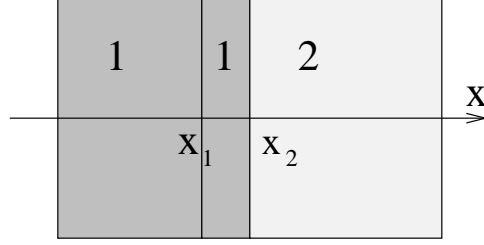


FIGURE 5. Model the effect of skin depth on temperature rise. Number 1 and 2 denote metal and diamond respectively.

$$T(x_2, t) = \frac{1}{1 + Z_2/Z_1} \frac{1}{\sqrt{\pi K_1 \rho_1 C_{v1} t}} e^{-\Delta x^2/4D_1 t}. \quad (26)$$

The RF loss decays exponentially into the metal, $e^{-2\Delta x/\delta}$, where δ is the skin depth. Considering an arbitrary pulse, the surface temperature at the end of the pulse is

$$T = \int_0^{T_p} \frac{P_0 f(t)}{1 + Z_2/Z_1} \frac{dt}{\sqrt{\pi K_1 \rho_1 C_{v1} t}} \int_0^\infty \frac{2d\Delta x}{\delta} e^{-2\Delta x/\delta} e^{-\Delta x^2/4D_1 t}, \quad (27)$$

where $f(t)$ represents the temporal profile of the pulse. After integrating Δx , we obtain

$$T = \frac{1}{1 + Z_2/Z_1} \frac{2P_0 T_p}{\sqrt{\pi K_1 \rho_1 C_{v1} T_p}} \frac{\sqrt{\pi}}{\delta_s} \int_0^1 e^{4t'/\delta_s^2} \operatorname{erfc}(2\sqrt{t'}/\delta_s) f(T_p t') dt'. \quad (28)$$

where the scaled skin depth $\delta_s = \delta/\sqrt{D_1 T_p}$. In the case of a square pulse, The integration gives

$$T = \frac{1}{1 + Z_2/Z_1} \frac{2P_0 T_p}{\sqrt{\pi K_1 \rho_1 C_{v1} T_p}} [1 + \alpha_s], \quad (29)$$

where the skin effect correction factor

$$\alpha_s = -\frac{1}{4}\sqrt{\pi}\delta_s + \frac{1}{4}\delta_s\sqrt{\pi}e^{4/\delta_s^2}\operatorname{erfc}\left(\frac{2}{\delta_s}\right) \quad (30)$$

$$= -\frac{1}{4}\sqrt{\pi}\delta_s + \frac{1}{8}\delta_s^2\left[1 + \sum_{m=1}^{\infty} (-)^m (2m-1)!! \left(\frac{\delta_s^2}{8}\right)^m\right] \quad (31)$$

The first linear term of δ_s is the heat spread due to skin depth effect even without diffusion. It results in a lower surface temperature. The value of α_s is plotted in Fig. 6. For a skin depth of $0.22 \mu\text{m}$ and 16 ns pulse, $\alpha_s = -0.068$.

Taking another limit that skin depth is much greater than diffusion length, i.e. $\delta_s \gg 1$ or $T_p \ll 0.4 \text{ ns}$ at 91 GHz , Eq. 29 and 30 becomes

$$T = \frac{1}{1 + Z_2/Z_1} \frac{2P_0 T_p}{\rho_1 C_{v1} \delta} \left[\sqrt{\pi} - \frac{8}{3} \frac{1}{\delta_s} + O\left(\frac{1}{\delta_s^2}\right) \right]. \quad (32)$$

The heat is concentrated in a layer roughly equal to the skin depth and diffusion is small. In this region the surface temperature is approximately linear with pulse length T_p and the interior of the metal may be much hotter than the surface.

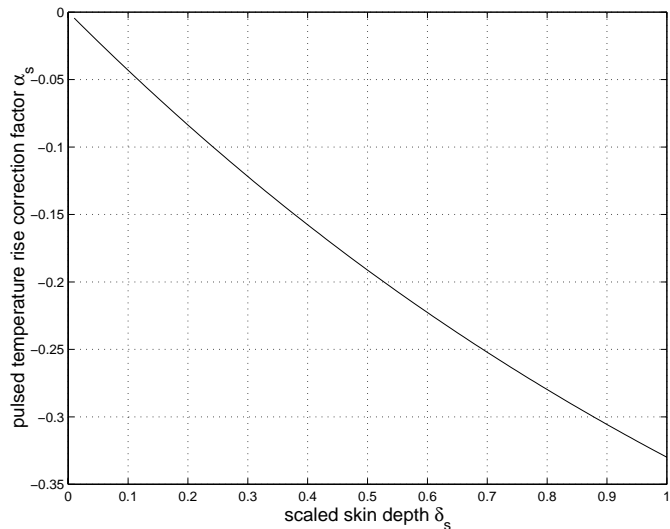


FIGURE 6. correction factor from skin effect.

D microwave property

Diamond not only has outstanding mechanical property, it is an excellent insulator with electric resistivity on the order of $10^{18} \Omega\text{m}$ and dielectric strength greater than 1 GeV/m [2] [3]. Its loss tangent $\tan \delta < 5 \times 10^{-4}$ is quite low. Thus for a pill-box cavity, the Q_d due to dielectric loss is approximately $l\epsilon'/\Delta x \tan \delta$, where l and Δx are the cavity length and coating thickness respectively. With a $8 \mu\text{m}$ coating in a $250 \mu\text{m}$ long cavity, $Q_d = 3 \times 10^5$. The dielectric loss is orders of magnitude smaller than metal wall loss.

E multi-layer structure

Taking advantage of the fact that diamond conducts heat better than copper. A three-layer system is proposed to reduce the pulsed temperature rise even further. Two advantages are realized here: First diamond conducts heat better than copper.

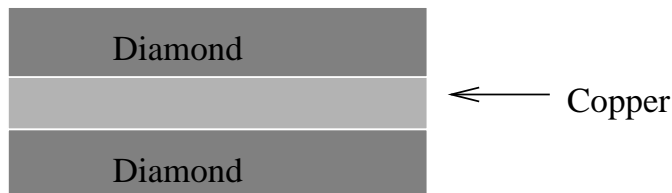


FIGURE 7. Three-layer configuration to reduce pulsed temperature rise.

Second heat generation is reduced by proper choice of metal thickness. The conduction current induced by the surface magnetic field decays exponentially inside metal; it also alternates direction with respect to the surface value because of the

phase lag. Choosing a film thickness of $0.345 \mu\text{m}$, about 1.57 times skin depth at 91 GHz, the reverse current is eliminated and RF loss is reduced by 8% [4].

Thin metal film on the order of skin depth $\sqrt{\omega\mu/2\sigma}$ provides excellent RF shielding due to almost perfect reflection at the metal-dielectric interface. For a coating thickness about 1.57 times skin depth, less than 2×10^{-4} of the total power loss leaks through metal film [4].

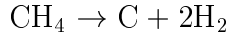
Taking the approximation that the metal film thickness is much smaller than the diffusion length, we can estimate the pulsed temperature rise from a point source in a medium of diamond, which gives

$$T = \frac{2P'_0 T_p}{\sqrt{4\pi K_2 \rho_2 C_{v2}}} = \frac{1}{2Z_2/Z_1} \frac{2P'_0 T_p}{\sqrt{\pi K_1 \rho_1 C_{v1} T_p}}, \quad (33)$$

where $P'_0 = 0.92P_0$. The two diamond layer configuration further reduces the pulse temperature rise to 0.26 times that of the bare copper.

III EXPERIMENT

We have chosen the microwave plasma enhanced CVD diamond process for its economy, deposition rate, lower temperature and good quality control [5]. Typically, methane and hydrogen mixture are introduced into the chamber. Under the microwave electric field, the gases are ionized into electrons and ions. The electrons, with their small mass, are quickly accelerated to high energy about a few thousands of degree or higher. The high energy electrons collide with gas molecules with resulting dissociation and generation of reactive chemical species and initiation of chemical reaction. The basic reaction is



The substrate must be heated to 800-1000° C for diamond to form because at lower temperature graphite is the thermodynamically stable allotrope. The resulting polycrystalline diamond has almost the same property as single crystal diamond.

The vastly different thermal expansion coefficient between Copper ($17 \times 10^{-6}/\text{K}$) and diamond ($1 \times 10^{-6}/\text{K}$) makes it very difficult to grow adherent and continuous diamond film on copper substrate. The fact that copper does not form carbide also makes adhesion extremely poor. The diamond film can usually be pulled off after the substrate is cooled to room temperature.

The key to growing diamond on copper is to find an appropriate interlayer that bonds well with copper as well as diamond. We have tentatively identified Titanium Tungsten which has excellent adhesion with copper substrate and form strong covalent bond with carbon. A proof of principle experiment at X-band is being pursued.

There is program at SLAC to look at the maximum pulsed temperature rise that copper can withstand [6]. A TE_{011} mode cavity with removable end plates is

powered by approximately $1.5 \mu\text{s}$ 20 MW of X-band (11.424 GHz) pulse. Hundreds of degrees surface temperature rise can be achieved. A removable end plate coated with $70 \mu\text{m}$ of diamond, corresponding to about 2 diffusion lengths in diamond of a $1.5 \mu\text{s}$ pulse, should be able to reduce the pulsed temperature rise to 36% that of bare copper end plate.

IV CONCLUSION

Pulsed temperature rise is likely the most severe restriction on the gradient in a structure based accelerator. Diamond coating to reduce pulsed temperature rise by a factor of 2.7 to 3.8 is possible if appropriate interlayer can achieve good adhesion. A proof of principle experiment is being carried out. Diamond coating also has important application in high power vacuum device, especially in the output cavities.

REFERENCES

1. S. Schultz, private communication.
2. L. S. Pan and D. R. Kania, "Diamond: electric properties and applications", pp 254.
3. K. E. Spear and J. P. Dismukes. "Synthetic Diamond: emerging CVD science and technology", pp 363.
4. Xintian E. Lin, "RF loss and leakage through thin metal film", submitted to IEEE transaction MTT.
5. H. O. Pierson, "Handbook of carbon, graphite, diamond and fullerenes", pp 302-321.
6. D. Pritzkau, *et al.* "Experimental study of pulsed heating of electromagnetic cavities", 1997 IEEE PAC.